Extension of the OFDM Joint Radar-Communication System for a Multipath, Multiuser Scenario

Yoke Leen Sit, Lars Reichardt, Christian Sturm, Thomas Zwick
Institut für Hochfrequenztechnik und Elektronik
Karlsruhe Institute of Technology
Karlsruhe, Germany
{leen.sit|lars.reichardt|christian.sturm|thomas.zwick}@kit.edu

***Abstract*—In this paper an extension of the OFDM joint radar and communication system concept to cope in a multipath and multiuser environment is explored. A realistic multipath propagation channel model is built with an established ray-tracing algorithm and incorporated into the radar system simulation and one additional user/interferer is then introduced into the scenario for the observation of the radar's performance. From a theoretical point of view as well as from measurement results, the interferer causes a severe degradation of the radar's dynamic range, thus requiring an interference cancellation scheme to remove the traces of the interferer. Inherent to the interference cancellation scheme is the phase and frequency offset estimation algorithm for the high fidelity reconstruction of the interferer signal for subtraction from the radar signal which are explored in this paper. The result of the end-system and the improvement to the radar's dynamic range are then presented.**

I. Introduction

An orthogonal frequency division multiplex (OFDM) joint radar and communication (RadCom) system concept based on the operation at 24 GHz has been proposed in [1][2]. The system uses OFDM communication signals as radar signals leading towards its dual role in object sensing and communication between systems. The novel radar processing method proposed is elegantly simple and completely independent of the transmitted information. Performance verification has also been done in [3] which made the concept feasible to be implemented in real systems. A typical application area for such systems would be in the intelligent transportation networks which require the ability of inter-vehicle communication as well as reliable environment sensing.

In extending the OFDM RadCom to a multipath-multiuser scenario, two major aspects have to be considered; namely a reliable channel model has to be taken into account, and impairment to the radar performance has to be countered. Firstly, a brief overview of the RadCom is presented in Section II. Next, a multipath propagation channel built using a ray-tracing algorithm and incorporated in the RadCom simulation is discussed in Section III. The introduction of an additional RadCom user is presented in Section IV. The impairment to the system is then countered by an interference cancellation scheme in Section V.

II. OFDM RadCom Concept

A symbol-based processing approach for range and Doppler processing has been proposed and implemented, contrary to the classical approach of cross-correlation. The RadCom system is considered for a channel where the coherence bandwidth is much larger than the subcarrier spacing. Cyclic prefixes (CP) are employed in the OFDM symbols to prevent inter-symbol interference (ISI). The parameterization of the OFDM RadCom frame taking into account the above said conditions is given in [4]. Each OFDM symbol consists of data modulated onto a set of orthogonal subcarriers. The resulting time domain signal (of one OFDM frame) can then be expressed as

$$x(t) = \sum_{\mu=0}^{M-1} \sum_{n=0}^{N-1} D\left(\mu N + n\right) \exp\left(j2\pi f_n t\right) \operatorname{rect}\left(\frac{t-\mu T}{T}\right) \tag{1}$$

with N denoting the number of subcarriers used, M, the number of consecutive symbols evaluated, f_n, the individual subcarrier frequency, T, the OFDM symbol duration, and $\{D(n)\}$, called the 'complex modulation symbol', is the arbitrary data modulated with a discrete phase modulation technique e.g. phase-shift keying (PSK). Interference between individual subcarriers is avoided based on the condition of orthogonality given by

$$f_n = n\Delta f = \frac{n}{T}, \qquad n = 0, ..., N-1 \tag{2}$$

In the presence of a reflecting object at the distance R from the RadCom with the relative velocity of v_{rel} which results in the Doppler frequency of f_D, the received OFDM symbol in time domain becomes

$$y(t) = \sum_{\mu=0}^{M-1} \sum_{n=0}^{N-1} D_r(\mu, n) \exp\left(j2\pi f_n t\right) \tag{3}$$

978-1-4244-8902-2/11/$26.00 ©2011 IEEE

where

$$D_r(\mu,n) = D(\mu,n)\exp\left(-j2\pi f_n \frac{2R}{c_0}\right)\exp\left(j2\pi f_D t\right) \quad (4)$$

Based on (4), it can be seen that the distortions due to the channel are fully contained in the received complex modulation symbols $\{D_r(\mu,n)\}$, which are obtained at the receiver at the output of the OFDM demultiplexer prior to channel equalization and decoding. Thus comparing the transmitted symbol $\{D(\mu,n)\}$ with the soft-side received symbol $\{D_r(\mu,n)\}$ would yield the time-variant frequency domain channel transfer function. This is computed by simply performing an element-wise division

$$I_{div}(\mu,n) = \frac{D_r(\mu,n)}{D(\mu,n)} \quad (5)$$

In this manner, the acquisition of the range and Doppler profiles will be independent of the payload data.

A. Range Processing

For an object at the distance R from the radar, all subcarriers within the same reflected OFDM symbol will experience a linear amount of phase shift equivalent to two times the time length taken to travel the distance R. Assuming that the object is stationary, the corresponding channel transfer function is

$$I_{div}(n) = \exp\left(-j2\pi n\Delta f \frac{2R}{c_0}\right), \qquad 0 \le n \le N-1 \quad (6)$$

The channel impulse response containing the range profile of the object can then be determined by taking an inverse discrete Fourier transform (IDFT) of $\{I_{div}(n)\}$

$$\begin{aligned} h(p) &= \mathrm{IDFT}\left(\{I_{div}(n)\}\right) \\ &= \frac{1}{N}\sum_{n=0}^{N-1} I_{div}(n)\exp\left(j2\pi\frac{n}{N}p\right), \qquad p = 0,...,N-1 \end{aligned} \quad (7)$$

B. Doppler Processing

Unlike with communication signals, the reflected radar signal of an object moving with a relative velocity of v_{rel} will experience twice the amount of Doppler shift according to

$$f_D = \frac{2\,v_{rel}}{\lambda} \quad (8)$$

where $\lambda = c_0/f_c$, with c_0 being the speed of light and f_c, the carrier frequency.

This causes a phase shift of $2\pi f_D \mu T_{sym}$ on every subcarrier of the μ-th OFDM symbol, where T_{sym} is the elementary OFDM symbol duration with its CP. It can be assumed that the Doppler affects all subcarriers by the same amount since the system bandwidth is much smaller than the carrier frequency. Thus for an object having a non-zero relative velocity to the radar, the corresponding time-variant channel transfer function (due to the Doppler only) is

$$I_{div}(\mu) = \exp\left(j2\pi f_D \mu T_{sym}\right), \qquad 0 \le \mu \le M-1 \quad (9)$$

By taking the discrete Fourier transform (DFT) through the time axis the Doppler term can be estimated.

$$\begin{aligned} h(q) &= \mathrm{DFT}\left(\{I_{div}(\mu)\}\right) \\ &= \frac{1}{N}\sum_{\mu=0}^{M-1} I_{div}(\mu)\exp\left(-j2\pi\frac{\mu}{M}q\right), \quad q = 0,...,M-1 \end{aligned} \quad (10)$$

Details of the system parameterization is discussed in [4] and is summarized in Table I.

TABLE I
OFDM SYSTEM PARAMETERS

Symbol	Parameter	Value
f_c	Carrier frequency	24 GHz
N	Number of subcarriers	1024
Δf	Subcarrier spacing	90.909 kHz
T	Elementary OFDM symbol duration	11 μs
T_{CP}	Cyclic prefix duration	1.375 μs
T_{sym}	Transmit OFDM symbol duration	12.375 μs
B	Total signal bandwidth	93.1 MHz
Δr	Range resolution	1.61 m
r_{max}	Maximum unambiguous range	1650 m
v_{max}	Maximum unambiguous velocity	$\pm$252.5 m/s
M	Number of evaluated symbols	256
Δv	Velocity resolution	1.97 m/s

III. MULTIPATH CHANNEL MODELING

Within a multipath environment, a certain transmitted signal will not only arrive at the receiver over the Line-of-Sight (LOS) path but also over Non-Line-of-Sight (NLOS) paths which interact in a complex manner with the objects (e.g. buildings, vehicles, persons, trees) within the propagation vicinity. These NLOS signals experience reflection, diffraction and scattering, resulting in their different attenuations, time delays, phase shifts and even polarizations. It is precisely due to the superposition of these NLOS signals that give rise to the frequency-selective, time-variant and direction-selective behavior of the mobile radio channel. As such, an accurate description of these multipath waves propagation in a given scenario is necessary to produce realistic time series of the channel impulse response.

For modeling the wave propagation in a multipath scenario, a three-dimensional fully polarimetric Ray-tracing algorithm developed by [5], [6], [7] is used. This channel model is based on Geometrical-Optics and describes the asymptotic behavior of the electromagnetic fields at high frequencies with the assumption that the wavelength is very small compared

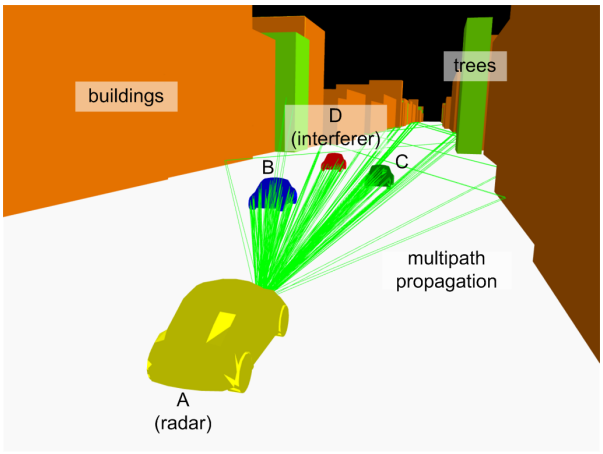

Fig. 1. Ray-tracing scenario

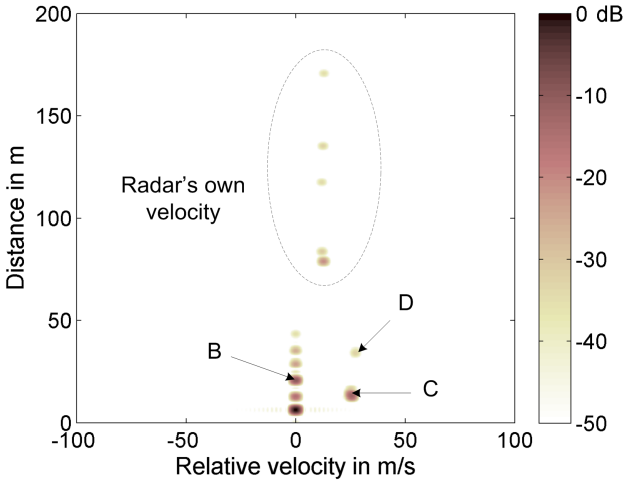

Fig. 2. Radar image of the ray-tracing scenario, single user

to the dimensions of the modeled objects in the simulation scenario. Each propagation path is represented by a ray which may experience several different propagation phenomena.

The 3D scenario for modeling the deterministic channel model is as shown in Fig.1. The green 'rays' depict the paths traveled by the electromagnetic waves. The 3D model of the cars is made up of around 700 triangles, each at least 25 cm^2, guaranteeing a large size relative to the wavelengths at 24 GHz which fulfill the requirements for using the ray-tracing algorithm. The model of the car is 3.8 m in length, 1.85 m in width and 1.7 m in height, with all perfect electrical conducting surfaces.

Channel Simulation

As depicted in Fig. 1 the investigated urban scenario comprises two lanes and four cars with buildings and vegetation on both sides of the street. Car A is performing the radar sensing and is thus denoted as the *radar*. Cars A and C are moving at the same direction with the set velocity v_{set}, of 12.9 m/s while B and D are moving at the opposite direction with the velocities of -13.3 m/s and -14.5 m/s respectively. The distances R, calculated from the center point of the cars of B, C and D from A are 16.4 m, 26 m, and 34.6 m respectively.

Two antennas, one transmit and one receive, are affixed on the bumper of car A and both have the characteristics of covering 90° in the azimuth and 180° in elevation (to take into consideration the reflections from the ground). With all the settings as described, one 'snapshot' is taken from the scenario. This snapshot contains all the paths of the rays including the amplitude, phase, Doppler and time delay of one OFDM frame of M symbols to be evaluated, and is exported to the complete RadCom system in MATLAB where one OFDM frame is evaluated. The resulting radar image is as shown in Fig. 2.

The detected range and relative velocities are as summarized in Table II. It can be seen that the simulated and set values have a slight difference. This is due to the fact that the reflective centers of the cars are not exactly at their center. Therefore a detection difference of within ±1.9 m (equivalent to half the length of the car) is considered as an accurate localization

TABLE II
RAY-TRACING SIMULATION DATA

Object	Settings			Simulation	
	R [m]	v_{set} [m/s]	v_{rel} [m/s]	R [m]	v_{rel} [m/s]
A	0	12.9	0	-	-
B	16.4	-13.3	26.2	16.1	25.7
C	26	12.9	0	25.2	0
D	34.6	-14.5	27.4	34.4	27.4

of the moving car. The object images at above 60 m are reflections from buildings along the road, and they depict the velocity at which the radar is traveling. Any objects other than the ones mentioned are the ground reflections. By adjusting the antenna elevation characteristics, the detection of the ground reflections can also be reduced.

IV. MULTIUSER SCENARIO

Within the created multipath environment, one additional user of the RadCom system concept transmitting a message-radar signal, also with multipath possibility is enabled in car D. This other user is henceforth denoted as the *interferer*. The analysis of the multiuser scenario is made from the view point the *radar*.

The radar receive power due to one reflecting object in its surrounding is given by the radar equation:

$$P_{radar} = P_t\, G_t\, G_r \left(\frac{\lambda}{4\pi}\right)^2 \frac{\sigma}{(4\pi)\, R_{obj}^4} \qquad (11)$$

where P_t, G_t and G_r are the transmit power, transmit antenna gain and receive antenna gain respectively, σ is the radar cross section (RCS) of the reflecting object and R_{obj} is the distance of the reflecting object to the radar.

The Friis equation gives an estimate of the interferer power received at the radar:

$$P_{interferer} = P_t\, G_t\, G_r \left(\frac{\lambda}{4\pi}\right)^2 \frac{1}{R_{int}^2} \qquad (12)$$

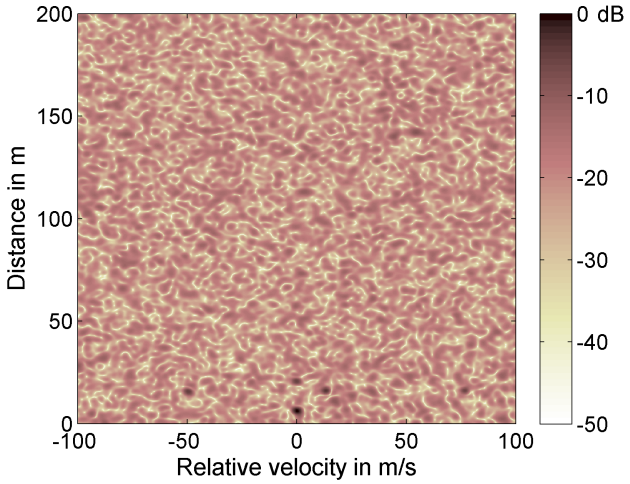

Fig. 3. Radar image of the ray-tracing scenario, before interference cancellation

where R_{int} is the distance of the interferer to the radar.

The signal-to-interferer ratio (SIR) at the radar can be estimated by taking the ratio of the receive power due to the reflecting objects in the radar's surrounding (radar equation) and the receive power due to the interferer (Friis equation), which gives:

$$SIR = \frac{R_{int}^2\,\sigma}{(4\pi)\,R_{obj}^4} \tag{13}$$

where R_{int} and R_{obj} are the distance of the interferer to the radar, and the reflecting object to the radar respectively, and σ is the RCS of the reflecting object. A reflecting object with 10 dBm^2 RCS located at 10 m, and the interferer at 50 m respectively from the radar would give an SIR of -7 dB. That is to say, the interferer signal is almost always higher than the reflected radar signal (even though the reflecting object is located nearer the radar) and hence appears as noise in the radar image, impairing the dynamic range.

From the ray-tracing results, the SIR is -30.2 dB and the strongest multipath component of the interferer is about 10 dB weaker than its LOS. The resulting radar image for the scenario of Fig. 1 is as shown in Fig. 3 where the mean noise floor is at -22.6 dB while the dynamic range (peak-to-sidelobe level) is a mere 6.8 dB. Consequently no distinguishable object reflection is visible in the radar image.

V. Interference Cancellation

As can be seen in Fig. 3, the communication signals end up as noise on the radar image. Since the radar also has access to the communication data, with a near-precise reconstruction of the interfering signal as received, this signal can then be subtracted from the radar signal.

In order to obtain an adequate reconstruction of the interfering signal, good time and frequency synchronization as well as channel estimation are necessary. For the purpose of time and frequency synchronization, the Schmidl and Cox algorithm (SCA) [8] has been implemented. The OFDM frame is thus extended by the length of two symbols, which does not cause any impairment to the radar's ranging capabilities.

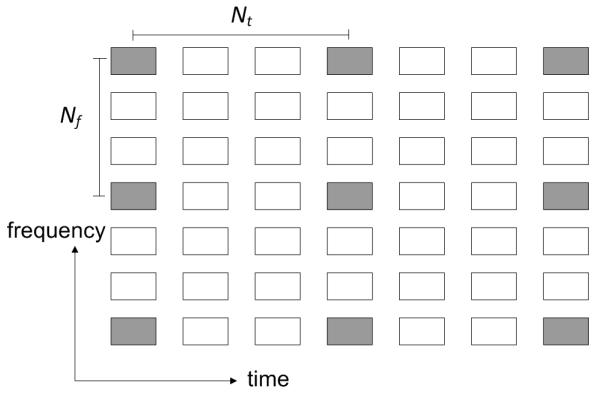

Fig. 4. Pilot symbol distribution within one OFDM frame

A. Interfering signal detection

The detection process begins with the identification of the strongest signal by the SCA algorithm through correlation. This signal is then time and frequency synchronized based on the estimation outcome of the SCA.

B. Channel estimation

The channel estimation is done by having regularly distributed pilot symbols within the OFDM frame where the phase rotation and amplitude attenuation of the symbols can be estimated. The spacing between the pilot symbols within the OFDM frame in the frequency axis is N_f, and in the time axis, N_t, is as shown in Fig. 4 and is given by

$$N_f \leq \frac{1}{\tau_{max}\Delta f} \tag{14}$$

$$N_t \leq \frac{1}{2f_{D_{max}}T_{sym}} \tag{15}$$

where τ_{max} is the time length for the longest path traveled by the signal in a multipath channel and it is assumed that the duration is as long as the duration of the CP, therefore N_f is the fraction of $\frac{N}{CP}$.

With the preambles and CP removed, the synchronized baseband signal is transformed to the modulation symbol domain. The received pilot symbols are then extracted and element-divided with the known pilot symbols to give $P_{div_{channel}}$. This process leaves the pilot symbols with the amplitude attenuation and phase rotation terms besides some small frequency offset terms due to the imperfect frequency correction of the SCA (as will be explored in the next subsection). The $P_{div_{channel}}$ matrix is then interpolated to the size of the OFDM frame of $N \times M$ for an easy element-wise division with the received OFDM symbols for channel compensation.

It must be noted here that the channel compensation using $P_{div_{channel}}$ is done *after* the fine frequency offset estimation

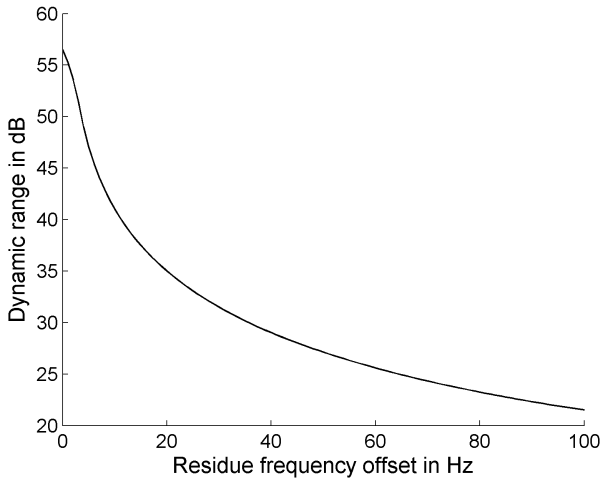

Fig. 5. Dynamic range (after interference cancellation) vs. residue frequency offset

in Section V-C. This step has been mentioned first because the fine frequency offset estimation requires the extraction of the pilot symbols as has been done in this step.

C. Fine frequency offset estimation

It has been observed that in a multipath-multiuser environment that when the LOS or strongest signal is less than 15 dB in difference with other NLOS and reflected signals, the SCA is incapable of estimating the precise frequency shift. This 'coarse' frequency correction is adequate for a correct PSK demodulation of the message signal but is inadequate in the reconstruction of the interfering signal for subtraction. The severity of erroneous frequency offset estimation on the reconstruction of the interfering signal is such that the difference of a mere 20 Hz from the real frequency offset will cause a degradation of more than 20 dB to the radar's dynamic range, as can be seen in Fig. 5. Thus a fine frequency offset estimator based on the evaluation of the pilot symbols in the previous step has been developed.

The received signal at the radar with one interfering signal, modified from (3) becomes

$$\begin{aligned} y(t) = &\sum_{\mu=0}^{M-1}\sum_{n=0}^{N-1} D_r(\mu,n)\exp\left(j2\pi f_n t\right) \\ &+ \sum_{\mu=0}^{M-1}\sum_{n=0}^{N-1} G_{r_i}(\mu,n)\exp\left(j2\pi f_n t\right) + n(t) \end{aligned} \tag{16}$$

where

$$\begin{aligned} G_{r_i}(\mu,n) = G_i(\mu,n)\exp\left(-j\left(2\pi f_n \frac{R_i}{c_0} - \varphi_i\right)\right)\cdot \\ \exp\left(j2\pi\delta\mu T_{sym}\right), \qquad i = 1,...,\infty \end{aligned} \tag{17}$$

where G_{r_i} and G_i are the i-th received and original interfering symbols respectively, R_i is the distance between the interferer or signal path with the radar, φ_i is the phase difference with the radar's reflected signal, and δ is the total frequency offset due to the Doppler and local oscillator (LO) difference between the interferer and the radar, and $n(t)$ is the noise. This frequency offset of δ causes the condition of 'loss of orthogonality' due to the misalignment of the interferer's and receiver's subchannels, leading to inter-carrier interference [9].

The first exponential term in (17) can be corrected to a good degree with the channel estimation using the pilot symbols. The second exponential term can only be partially corrected by the SCA depending on the strength of the LOS signal power thus leaving behind a residue frequency offset term.

Here it is assumed that the SCA performed an adequate 'coarse' frequency offset compensation which minimizes the inter-symbol interference (ISI) term to a negligible value, and perfect channel compensation is done in which the symbols can be correctly demodulated. Hence in the modulation symbol domain, the residue frequency offset term can be written as

$$H(\mu,n) = \exp\left(j2\pi\epsilon T_s \mu N\right), \qquad n = 0,...,N-1 \tag{18}$$

where ϵ is the residue frequency offset uncorrected by the SCA and T_s is the sampling time given by $\frac{T}{N}$. This expression takes into account the serial to parallel conversion of the OFDM symbols at the receiver and the removal of the preambles and CP before the DFT process. Thus it can be seen that there exists an exponential term independent of the subcarrier index (which is associated with the inter-symbol interference term), and can be used to determine the frequency offset in a way similar to (10). The effect of this residue frequency offset on every OFDM symbol including the pilot symbols is given by

$$\tilde{G}_i(\mu,n) = \exp\left(j2\pi\mu\epsilon T\right) G_i(\mu,n) \tag{19}$$

Hence, retrieving only the pilot symbols in the communication signal $Z_p(\mu,n)$, and performing element-wise division with the known pilot symbols $P_{known}(\mu,n)$, would leave only the exponential term in (19) intact.

$$P_{div}(\mu,n) = \frac{Z_p(\mu,n)}{P_{known}(\mu,n)} \tag{20}$$

$P_{div}(\mu,n)$ is then interpolated to the size of the OFDM frame of $N \times M$. Taking a DFT of $P_{div}(\mu,n)$, the term will be maximum at $\psi = \epsilon T M$ and the residue frequency offset ϵ can be found.

$$\begin{aligned} \mathrm{DFT}\left(\{P_{div}(\mu)\}\right) = \sum_{\mu=0}^{M-1} Z(\mu,n)\exp\left(-j2\pi\frac{\mu}{M}\psi\right), \\ \psi = 0,...,M-1 \end{aligned} \tag{21}$$

The accuracy of the frequency offset residue is dependent on the number of pilot symbols evaluated and is given by

$$\eta = \frac{1}{\alpha M T_{sym}} \tag{22}$$

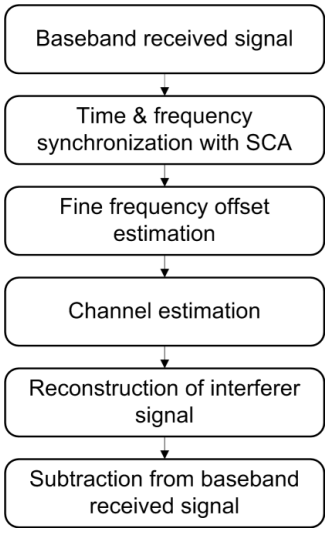

Fig. 6. Flow diagram of the interference cancellation

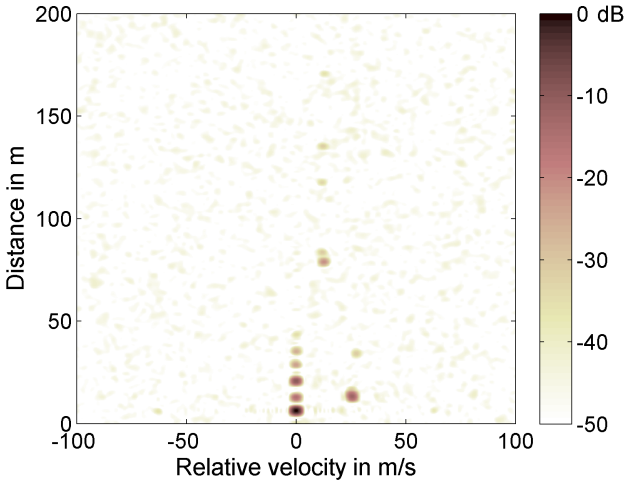

Fig. 7. Radar image after interferer's LOS component cancellation

where α is the zero padding factor that increases the resolution of the residue frequency offset estimate. In this manner, the residue frequency offset estimator is capable of estimating the residue frequency offset ϵ to the precision of $\frac{\eta}{2}$ and below.

D. Interferer reconstruction and subtraction

In the reconstruction of the strongest detected interfering signal (LOS) to the state as it was received, the interferer detection process is reversed. The channel effects are added to the message modulation symbols by a simple element-wise multiplication with $P_{div_{channel}}$. Then the total frequency offsets estimated from the SCA and fine frequency offset estimator are added. The signal is then shifted in time domain reversing the process of the SCA time synchronization. The flow of the interference cancellation scheme is summarized in Fig. 6.

This recontructed interfering signal is then subtracted from the baseband received signal. Shown in Fig. 7 is the resulting radar image after interference cancellation of the interferer's LOS path, where the residue frequency offset amounts to only 0.18 Hz and the mean noise floor is now at -53 dB along with 40.7 dB of dynamic range (peak-to-sidelobe ratio). With this, all reflecting objects in the path of the rays are visible.

VI. Conclusion

In the regarded step for extending the RadCom concept to function in a multipath-multiuser environment, the challenges of the realistic multipath scenario setup and the implication of one other user in the radar's vicinity have been discussed. It has also been shown that the interfering signal severely corrupts the radar's dynamic range. Hence an interference cancellation scheme using the availability of the received communication signal to the radar has implemented. This interference cancellation scheme utilizes information extracted from the regularly spaced pilot symbols within the OFDM frame. The simple fine frequency offset estimator then extracts the frequency offset information from the channel estimation matrix and is capable of significantly reducing the frequency offset error in the reconstructed signal. Implementing the interference cancellation algorithm, the performance of the radar is seen to improve by around 34 dB after the cancellation of the strongest (LOS) path of the interferer.

References

[1] C. Sturm, T. Zwick, and W. Wiesbeck, "An OFDM System Concept for Joint Radar and Communications Operations," in *Vehicular Technology Conference, 2009. VTC Spring 2009. IEEE 69th*, Apr. 2009, pp. 1 –5.

[2] C. Sturm, M. Braun, T. Zwick, and W. Wiesbeck, "A Multiple Target Doppler Estimation Algorithm for OFDM based Intelligent Radar Systems," in *Proceedings 7th European Radar Conference, Paris, France*, Sep. 2010.

[3] C. Sturm, T. Zwick, W. Wiesbeck, and M. Braun, "Performance Verification of Symbol-based OFDM Radar Processing," in *Radar Conference, 2010 IEEE*, May. 2010, pp. 60 –63.

[4] M. Braun, C. Sturm, A. Niethammer, and F. Jondral, "Parametrization of Joint OFDM-based Radar and Communication Systems for Vehicular Applications," in *Personal, Indoor and Mobile Radio Communications, 2009 IEEE 20th International Symposium on*, Sep. 2009, pp. 3020 –3024.

[5] J. Maurer, "Strahlenoptisches Kanalmodell für die Fahrzeug-Fahrzeug Kommunikation," Ph.D. dissertation, Institut für Hochfrequenztechnik und Elektrotechnik, Universität Karlsruhe (TH), May 2005.

[6] T. Fügen, J. Maurer, T. Kayser, and W. Wiesbeck, "Capability of 3-D Ray Tracing for Defining Parameter Sets for the Specification of Future Mobile Communications Systems," *Antennas and Propagation, IEEE Transactions on*, vol. 54, no. 11, pp. 3125 –3137, Nov. 2006.

[7] L. Reichardt, T. Schipper, and T. Zwick, "'Virtual Drive' Physial Layer Simulation for Vehicle-to-Vehicle Communications," in *Proceedings of the 2010 International Symposium on Electromagnetic Theory EMTS2010, Berlin, Germany*, Aug. 2010.

[8] T. Schmidl and D. Cox, "Robust Frequency and Timing Synchronization for OFDM," *Communications, IEEE Transactions on*, vol. 45, no. 12, pp. 1613 –1621, Dec. 1997.

[9] J. Armstrong, "Analysis of New and Existing Methods of Reducing Intercarrier Interference due to Carrier Frequency Offset in OFDM," *Communications, IEEE Transactions on*, vol. 47, no. 3, pp. 365 –369, Mar. 1999.